Cloning and characterization of murine carnitine acetyltransferase: evidence for a requirement during cell cycle progression

Sylvia BRUNNER*, Konrad KRAMAR*, David T. DENHARDT† and Reinhold HOFBAUER*‡

*Institut für Molekularbiologie, Wiener Biozentrum, Universität Wien, Dr. Bohrgasse 9, A-1030 Wien, Austria, and †Nelson Biological Laboratories, Department of Cell, Developmental and Neurobiology, Rutgers University, Piscataway, NJ 08855-1059, U.S.A.

We have employed a newly developed differential screening technique (reverse strand priming) to identify murine carnitine acetyltransferase (CARAT) as a growth- and cell cycle-regulated gene in S3T3 mouse fibroblasts. Sequence analysis of the full-length cDNA clone and homology comparisons have revealed 87% homology to the human CARAT gene. On Northern blots we were able to measure a 2–3-fold induction 18 h after a mitogenic stimulus following serum deprivation as well as after release from a sodium butyrate block. The cell cycle induction pattern of the CARAT gene was analysed in mouse fibroblasts at different stages of the unperturbed cell cycle. Fractions obtained by elutriation of an exponentially growing culture showed a biphasic maximum of transcript abundance in the G1 and G2 phases of the cell cycle. CARAT expression was investigated in several organs of the adult mouse. Among those measured, CARAT expression was highest, relative to liver, in heart muscle (56-fold) and testis (21-fold). Using both conventional antisense oligodeoxynucleotides and novel single-stranded antisense phagemid DNA, we obtained evidence that the CARAT enzyme function is necessary for progression through G1 and into the S-phase of the cell cycle.

INTRODUCTION

Carnitine acetyltransferase (CARAT) (EC 2.3.1.7) belongs to a family of closely related and highly conserved transferases that transfer acyl groups of different sizes from acyl-CoA to L-carnitine [1,2]. A number of members of this family expressed in several species and tissues have been cloned [3–11]. Carnitine and CARATs are involved in several pathological processes. In animals, pharmacological studies involving administration of acetylcarnitine showed that energy production could be enhanced and that age-related degenerative membrane alterations could be reverted. In aged rats acetylcarnitine was able to increase the rate of mitochondrial replication to that measured in juvenile animals [12].

There are a variety of pharmacological reasons to subject the CARAT enzyme to further analysis. These include its involvement in eukaryotic mitochondrial acyl group transfer as a building block for fatty acid biosynthesis [13] and its close functional and genetic relationship to the carnitine palmitoyltransferase (CARPT). In patients suffering from CARAT deficiency, serious neurological, motor, respiratory and heart problems were observed which underline the importance of an undisturbed CARAT function [14,15]. The importance of CARPTs is convincingly demonstrated by inherited deficiencies of CARPT activity in humans, which result in hypoketonaemia and hypoglycaemia [16–19]. Non-insulin-dependent diabetes probably could be treated with inhibitors of CARPT-1 (e.g. Etomoxir), because blood glucose levels can be lowered when these compounds are administered [20,21]. Analysis of tissue samples from the brains of deceased Alzheimer's disease victims revealed 'abnormal' energy production, which was associated with cell death and membrane destruction, and which increased with the severity of the disease. CARAT activity was decreased in Alzheimer's disease brain autopsies by about 25–40% compared with normal brain enzyme activity levels [22–24].

Here we present a molecular analysis of the full-length murine CARAT cDNA, which we have cloned by differential screening of synchronized S3T3 cells in late G1 versus cells in mid S-phase [25,26]. We were able to isolate this cDNA in our differential screen because of its up-regulation after a mitogenic stimulus following growth arrest induced by the metabolic blocker sodium butyrate [27]. To define the possible biological significance of a novel cDNA clone emerging from a differential screen, it is useful to make a prior assessment of potential function. To accomplish this, we have developed a novel approach by performing inhibition studies with sense and antisense CARAT-specific sequences encoded by single-stranded DNA phagemids. These experiments demonstrated that the progression of the cell towards S-phase was dependent on the proper induction of CARAT transcripts and on normal translation into functional protein. A significant loss of growth potential as measured by thymidine incorporation into newly synthesized DNA was the consequence of antisense-induced reduction of CARAT expression.

MATERIALS AND METHODS

Cell culture, growth arrest and stimulation of cell populations

S3T3 (ATCC CCL-92) and NIH3T3 mouse fibroblasts (ATCC CRL-1658) were grown in Dulbecco's modified Eagle's medium (DMEM) containing 10% foetal-calf serum (FCS) and anti-

Abbreviations used: CARAT, carnitine acetyltransferase; CARPT, carnitine palmitoyltransferase; DEPC, diethylpyrocarbonate; DMEM, Dulbecco's modified Eagle's medium; FCS, foetal calf serum; GAPDH, glyceraldehyde phosphate dehydrogenase; GST, glutathione S-transferase; hTK1, human thymidine kinase 1; IPTG, isopropyl β-D-thiogalactopyranoside; ODN, oligodeoxynucleotide, PCI, phenol/chloroform/isoamyl alcohol (25:25:1, by vol.); RSP, reverse strand priming.

The complete nucleotide sequence of the murine CARAT cDNA clone (MMRNACAR) is deposited in the EMBL data bank under the accession number X85983.

‡ To whom correspondence should be addressed.

biotics (30 mg/l penicillin, 50 mg/l streptomycin sulphate). For starvation, cells were kept in DMEM containing 0.2 % FCS for 72 h. Growth induction was performed by adding fresh DMEM containing 20 % serum for different periods of time as indicated by the time course protocol. Growth arrest by sodium butyrate administration was achieved by adding 6 mM sodium butyrate, pH 7.4, to the complete medium (10 % serum) for 18 h. The subsequent release of the drug inhibition was done by removal of the inhibitor-containing medium followed by a washing step with PBS and a final incubation in fresh medium containing 10 % FCS. The proliferative growth state of cell populations was assessed by a Partec PAS-2 cytofluorimeter measuring the DNA content. Centrifugal elutriation of exponentionally growing NIH3T3 cells (usually 3×10^8 cells/centrifugation) was performed using Beckman elutriation equipment.

Sense/antisense inhibition experiments

The sense/antisense 18-mer oligodeoxynucleotide (ODNs) were delineated from the primary sequence of our first but partial CARAT cDNA clone just after an ATG of the predicted open reading frame (RH3, 5′-GGATCCTAACCTCCAACC, corresponding to nt 873–892 of the full length murine CARAT cDNA; its complementary counterpart was RH4, 5′-GGTTGGAGGTTAGGATCC, antisense to RH3). Single strand phagemids (SK + and SK −) carrying the complete cDNA were rescued from pBluescript-CARAT-cDNA carrying bacteria by super infection with f1 helper phages R408 [28] or VCSM13 (Stratagene) and quantified by gel electrophoresis and densitometric analysis [26]. Subsequent sonication was optimized to generate an average fragment length of 0.25 kb. Increasing amounts of sequence- and strand-specific phagemid DNA or ODNs were added to synchronized or exponentionally growing S3T3 cell populations (10^5 cells/5-ml cell culture plates). After specific intervals a [^{3}H]thymidine pulse label was performed for 30 min to label the nascent DNA. Termination of incorporation and extraction of the labelled DNA was achieved by precipitation with trichloroacetic acid and scintillation counting of the acid-insoluble [^{3}H]thymidine.

Reverse strand priming (RSP) and differential screening

The sensitivity achieved by differential hybridization is a function of the specific activity of the cDNA probe. To improve the sensitivity we employed the following procedure, which is called RSP and was described in more detail previously [26]. The first cDNA synthesis step was performed under optimal conditions (0.6 mM for all four dNTPs [29]) for the production of full-length transcripts, which in this case averaged about 3 kb when murine poly(A*)$^+$ mRNA was used. Radioactive label was then introduced by random hexanucleotide priming [30] using the single-stranded cDNA as a template and the Klenow fragment of DNA polymerase I. This yielded a specific radioactivity of 10^8–10^9 c.p.m./μg of DNA, almost 10^3 more than the conventional method where the radioactivity was directly incorporated by the reverse transcriptase during first-strand synthesis [31].

In a typical cDNA synthesis we split the reaction mixture for the single-strand cDNA in two unequal portions. For one-third (using approx. 2 μg of cDNA) the reaction was performed in the presence of 5 μl of [α-^{32}P]dCTP (650 Ci/mmol) in order to monitor the reaction and to analyse the products on an agarose gel. The remaining two-thirds of the first strand reaction was saved for later labelling (second screen) or for library synthesis reactions. Prior to the random hexamer-driven labelling reaction of the cDNAs from the two RNA preparations to be compared, the single-stranded cDNA was treated with 0.3 M NaOH for 1 h at 65 °C to degrade the template mRNA. The subsequent labelling reaction was performed with an aliquot not exceeding 50 ng of single-stranded cDNA. The unlabelled first-strand cDNAs for the differential hybridization experiments were quantified by photometric or fluorimetric measurement and subsequently after labelling by agarose gel electrophoresis. The specific incorporation was measured by scintillation counting of trichloroacetic acid-precipitable DNA. For the differential screening it is critical to use equivalent amounts of equivalently labelled DNA for the hybridization experiment.

Conditions for differential hybridization and identification of the mouse CARAT cDNA clone

Approximately 4×10^3 phages per 15-cm Petri dish were plated. Plaques were lifted and blotted on nitrocellulose filters according to standard methods [31]. Prehybridization was performed for 16–18 h at 42 °C in a solution containing 40 % formamide, 5 × SSC, 10 × Denhardt's solution, 50 μg/ml poly(dA), 0.1 % SDS, and 100 μg/ml sonicated denatured salmon sperm DNA. For subsequent hybridization the random labelled cDNA probes were added to the hybridization containers and the incubation was continued for an additional 36 h at 42 °C. The plaque lift filters were washed with the desired stringency and then exposed to an X-ray film for 3 days. The positive plaques were replated in suitable dilutions and rehybridized with the differentially labelled cDNA probes to exclude false positive plaques and contaminants. In order to obtain full-length clones, cDNA clones of the partial cDNAs identified by the differential screening were labelled and used to rescreen the S3T3 cDNA library described above, which was especially tailored to harbour full-length cDNA clones; conditions were optimized for the production of full length transcripts, and size fractionation of the double-strand cDNA was performed before cloning into lambda.

RNA extraction and Northern blot analysis

To isolate cytoplasmic RNA, 3×10^7 cells, either harvested from Petri dishes by trypsinization or collected from fractions after centrifugal elutriation, were washed twice with PBS, resuspended in 200 μl of ice-cold buffer A (10 mM Hepes, pH 7.9/10 mM KCl/0.1 mM EDTA/0.1 mM EGTA/2.5 mM dithiothreitol), and combined with 10 μl of 12.5 % Nonidet P40. After shaking for 10 s the suspension was centrifuged at 15000 ***g*** at room temperature for 2 min. The supernatant was pipetted into a tube with 400 μl of buffer B (7 M urea/1 % (w/v) SDS/0.35 M NaCl/10 mM EDTA) and 400 μl of PCI (phenol/chloroform/isoamyl alcohol, 25:25:1, by vol.). The probes were vortexed and stored at −20 °C. After 30 min centrifugation at 4 °C (2000 ***g***) the aqueous phase was precipitated with two volumes of ethanol. Following a washing step with 70 % ethanol, the RNA was dissolved in diethyl pyrocarbonate (DEPC)-treated water.

RNA was isolated from mouse organs using the GTC method (RNAgents™ Total RNA Isolation Kit, Promega). The tissue was disrupted on ice in the appropriate volume (12 ml/g of tissue) of GTC solution (4 M guanidine thiocyanate/25 mM sodium citrate, pH 7.0, 0.5 % sarcosine, 100 mM β-mercaptoethanol) in a Dounce homogenizer. After addition of 0.1 vol. of sodium acetate (2 M, pH 4.0) the suspension was mixed by inversion. Water-saturated phenol (1 vol.) was added, vigorously shaken for 15 s and then chilled on ice for 15 min. After centrifugation (4 °C, 10000 ***g***, 30 min) the upper aqueous phase was transferred to a new tube and precipitated with an equal

volume of propan-2-ol. The pellet was washed with 70% ethanol and dissolved in GTC-solution again (10 min at 40 °C) to repeat the extraction. After a third extraction, the RNA was resuspended in DEPC-treated water.

The RNA (10 μg) was fractionated on denaturing 1% agarose gels containing 4% formaldehyde, transferred to GeneScreen nylon membranes (Du Pont–New England Nuclear) and cross-linked to filters by ultraviolet light. Staining of the membranes with Methylene Blue was performed by rinsing the membrane in distilled water and then staining in Methylene Blue solution (0.04% Methylene Blue/0.5 M sodium acetate adjusted to pH 5.2) for 10 min and subsequent partial destaining with distilled water.

Mouse CARAT cDNA was radiolabelled by random priming (random priming kit, Amersham) and used as a probe. The filter was hybridized overnight at 42 °C in 50% formamide, 5 × SSPE (0.15 M NaCl/10 mM sodium phosphate, pH 7.4/1 mM EDTA)/0.1 M sodium phosphate, pH 6.5/5 × Denhardt's/10 mM EDTA, pH 8.0/1% Sarkosyl/100 μg/ml yeast tRNA. The final wash was in 2 × SSC/0.1% SDS at 65 °C. An ODN (5′-CCCGCCGGGCTCCCCGGG; nucleotides 3046–3063 of 28 S rRNA) and rat GAPDH (glyceraldehyde phosphate dehydrogenase) cDNA were used as controls for the relative amounts of RNA. The ODN was end-labelled with [γ-^{32}P]ATP (3000 Ci/mmol, New England Nuclear) as described earlier [31].

Cloning of the CARAT cDNA into pGEX-2TK-MCS and isolation of a fusion protein

The subcloning was done by PCR amplification of the CARAT cDNA (according to standard protocols with Vent DNA polymerase, New England Biolabs) and subsequent cloning into pGEX-2TK-MCS [32,33]. The sense ODN (5′-AGA CAT CGA TCA TGT TAG CCT TTG CT) contains the initiating ATG and a *Cla*I site for subcloning. The antisense ODN (5′-TGG GCC TCG AGT CAG AGC TTG GCC CT) contains the stop codon and an *Xho*I site for subcloning. The CARAT–fusion protein was synthesized in *Escherichia coli* DH5 α and purified according to standard protocols [34].

Biochemical and theoretical sequence analysis

Double-strand sequencing was performed with *Taq* polymerase (Promega) according to standard protocols distributed by the vendor and Sanger's dideoxy chain termination method [31]. Analysis of the primary sequence was done with Genetics Computer Group Sequence Analysis Software Package, Version 7.3.1-UNIX and by the programs contained in the PC GENE and the FASTA [35] software packages developed for PC-based computational methods.

RESULTS

We have utilized a very sensitive differential screening method which allowed us to identify cDNA clones of genes differentially expressed at low abundance during progression of eukaryotic cells from G1 towards S-phase of the cell cycle [26]. In this screen several hundred, potentially novel, growth stimulus responsive clones have been detected and sorted on the basis of their specific induction behaviour and stability in different phases after a proliferation stimulus [25]. Using cDNA transcribed under conditions where full-length transcripts were produced, followed by a random priming synthetic step utilizing the single-stranded cDNA, we were able to produce DNA labelled at a high specific radioactivity ($> 10^8$ c.p.m./μg of DNA). The differential hybridization was performed with transcribed and labelled cDNA isolated from S3T3 cells, comparing timepoints between mid-G1 versus the first half of S-phase. The mouse S3T3 cells were isolated 8 and 15 h after release from growth arrest caused by sodium butyrate, which is known to arrest fibroblasts in early G1 [27,36].

The final differential hybridization identified cDNA clones from a library established in λZAP II from S3T3 cells in S-phase. Clone 3-1a is one out of ten clones selected from the low-abundance clone collection (those that yielded a weak signal when probed with the 15 h reverse strand primed and labelled cDNA). It showed a strictly cell cycle-coupled regulation as well as a strong growth induction in serum-induced and butyrate-released S3T3 cells. All differentially regulated gene functions were subjected to a Northern-blot analysis to verify their specific induction pattern in serum-arrested (starvation versus sodium butyrate block) as well as in serum-induced cells and in unperturbed cells purified by centrifugal elutriation. The details of the synchronization and induction protocols are described in the Materials and methods section.

The sequence of the cDNA clone was determined and subsequently analysed by the GCG software package. The largest open reading frame coding for a 627-amino-acid-long predicted protein was compared with the existing data banks (EMBL, Genbank). Significant homologies to several mammalian carnitine acyltransferases were detected by the FASTA program, leading to the conclusion that cDNA clone 3-1a is a murine CARAT (87% homology to the human CARAT, 76.5% to porcine and 55% to *Drosophila melanogaster* choline acetyltransferase, 53% to carnitine palmitoyl and octanoyl transferase). These homology scores strongly argue that this enzyme function is coding for a G1/G2 specific cell cycle regulated CARAT function (comparisons all performed with the LFASTA program) [35]. A multiple alignment of the translated amino acid sequence of the murine CARAT to the other CARATs (human, pigeon, *Saccharomyces cerevisiae*) is presented in Figure 1 and graphically demonstrates the high degree of conservation even between distant eukaryotic species. The 2596 bp nucleotide sequence of the cDNA clone (MMRNACAR) is deposited in the EMBL data bank under the accession number X85983.

Figure 2 shows a typical Northern-blot analysis of the transcript abundance of clone 3-1a at different timepoints after serum induction and growth arrest compared with 8 h versus 15 h after sodium butyrate release. These are the two timepoints chosen for the differential hybridization analysis in Swiss S3T3 cells. Cytoplasmic mRNA and poly(A)$^+$ RNA were separated on a 1.2% agarose gel and subsequently hybridized with a randomly labelled 3-1a cDNA probe. Cycloheximide was added at the induced timepoint (15 h after sodium butyrate release); a superinduction of the CARAT mRNA is not caused by this drug. Since cycloheximide is able to prevent degradation of unstable transcripts, we could conclude that transcription rate and/or stabilization of the CARAT message are the reasons for the increase in transcript abundance [37]. At the 15 h timepoint we measured a 2.5-fold increase in CARAT transcript abundance compared with 8 h after butyrate release. The murine CARAT mRNA turned out to be a strictly growth-regulated gene function. In Figure 3 a complete growth cycle in NIH 3T3 cells after mitogenic stimulus is presented. In this cell culture, cells with the lowest transcript level can be measured at 4 h after growth induction with a relatively high-level CARAT mRNA content at 0 h compared with the corresponding timepoint in Figure 2. Afterwards a steady increase in CARAT mRNA is clearly visible, reaching 19-fold transcript enrichment after 24 h serum induction. High murine CARAT mRNA levels were also detected in

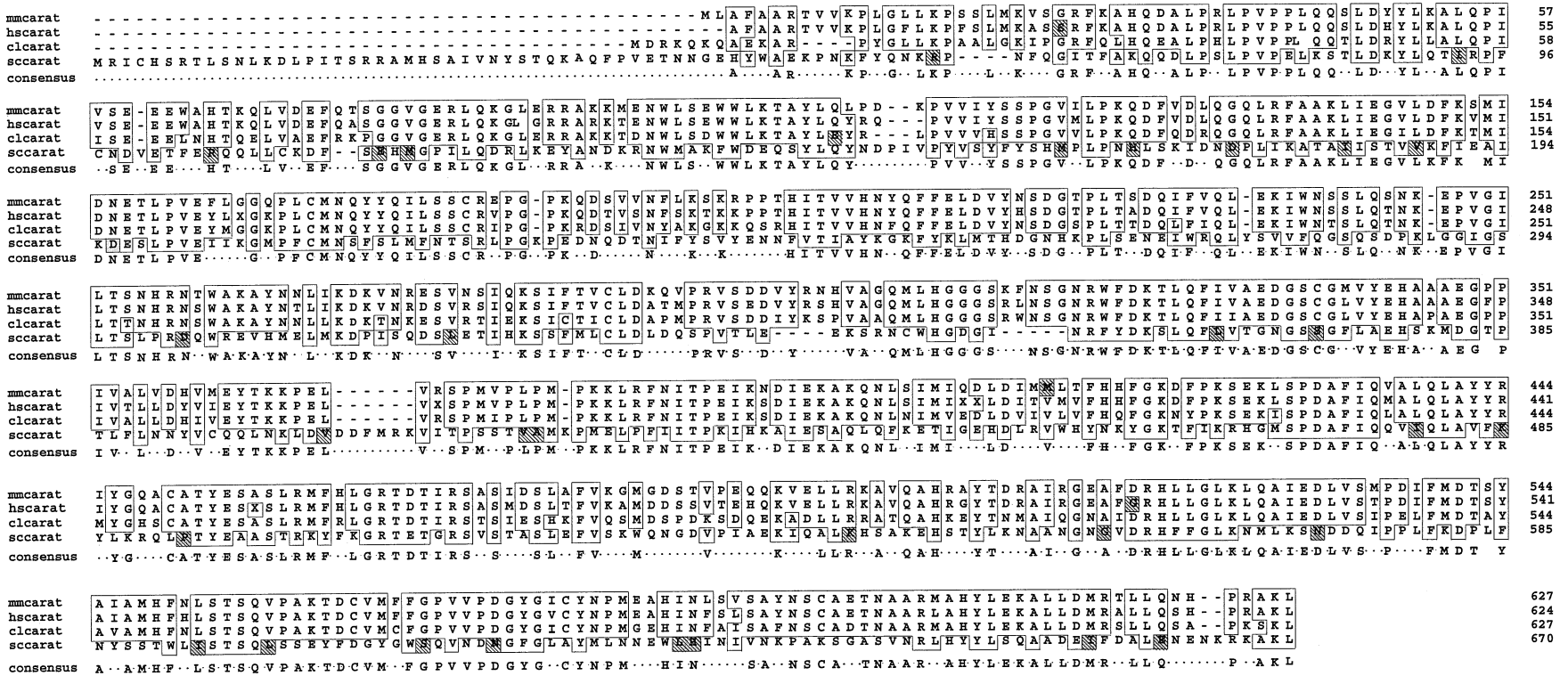

Figure 1 Sequence comparison of the deduced amino acid sequences from mouse, human, pigeon and yeast CARATs

The amino acid sequences from the murine (mmcarat), human (hscarat), pigeon (clcarat) and *S. cerevisiae* (sccarat) CARAT cDNA clones were aligned by the PRETTYPLOT and PRETTYBOX programs contained in the GCG DNA analysis package. The Figure represents a combination of both analyses. Conserved regions are boxed and conservative exchanges of amino acids are hatched and boxed. The resulting consensus sequence is printed underneath the alignments.

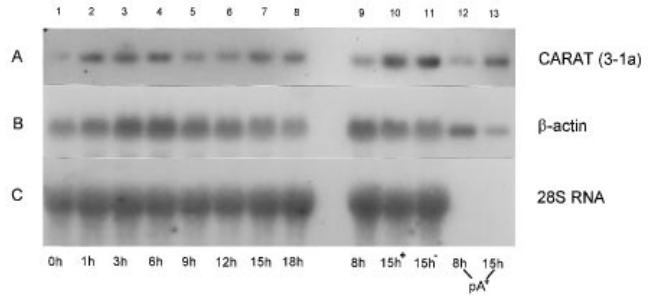

Figure 2 Northern-blot analysis of CARAT (clone 3-1a) mRNA levels after 8 and 15 h release of S3T3 fibroblasts from a butyrate block in comparison with a time course of growth-arrested and serum-induced S3T3 cells

Lanes 1–8, equal amounts (10 μg/lane) of cytoplasmic RNA isolated from cells arrested by serum deprivation for 72 h in a medium containing 0.2% FCS and subsequently induced with fresh medium containing 20% FCS for 0, 1, 3, 6, 9, 12, 15 and 18 h, respectively. Lanes 9–11, equal amounts (10 μg/lane) of cytoplasmic RNA isolated from cells 8 h and 15 h after release of a butyrate block. Lanes 12 and 13, [labelled p(A^+)] contain poly(A^+) RNA (1 μg/lane) from cultures 8 h and 15 h after release from butyrate arrest. All RNA samples were electrophoresed on a denaturing gel, blotted and hybridized with a random-primed CARAT cDNA (**A**), murine β-actin (**B**) and 28S RNA (C) probe. Lanes labelled 15^+ and 15^- represent RNA isolated from cells in the presence and absence of cycloheximide (10 mg/ml supplemented 2 h before RNA isolation). The control hybridization was performed with 28S RNA for all lanes with cytoplasmic RNAs (**C**). The visible weak serum induction of mouse β-actin after serum induction in (**B**) is in agreement with the published expression behaviour of this gene function. For both the cytoplasmic RNA and the poly(A^+) RNA the amount of CARAT mRNA at 15 h was about 3.5 times higher than in cells induced for 8 h.

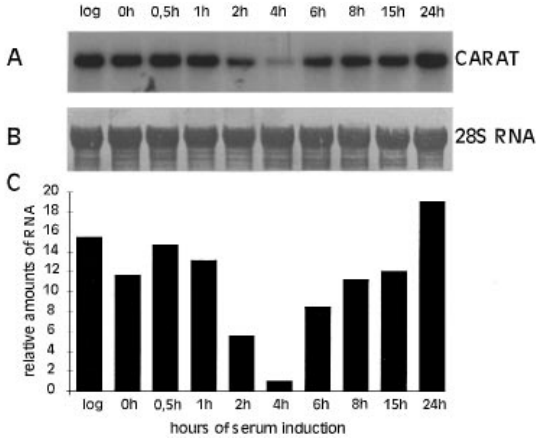

Figure 3 Northern-blot analysis of CARAT mRNA levels in exponentionally growing versus starved and serum-induced NIH3T3 mouse fibroblasts

Cytoplasmic RNA (10 μg) was fractionated on a denaturing gel, transferred and hybridized with random primed CARAT cDNA. The cells were synchronized by serum deprivation for 72 h in a medium containing 0.2% FCS. The cytoplasmic RNA was prepared from cells that were stimulated with medium containing 20% FCS for 0, 0.5, 1, 2, 4, 6, 8, 15 and 24 h. On the lane labelled 'log' cytoplasmic RNA from exponentionally growing cells has been loaded. The induction behaviour of the CARAT mRNA in NIH3T3 cells is presented in panel (**A**), which is slightly different from the kinetics of serum induction in S3T3 cells presented in Figure 2. But the biphasic expression pattern with peak levels of CARAT mRNA in early G1 and S/G2 is strictly conserved. The control is 28 S RNA (**B**), and (**C**) shows the amount of CARAT mRNA relative to 28 S RNA.

exponentionally growing cells and at earlier timepoints (< 4 h serum induction).

Subsequently we decided to analyse the CARAT transcripts when cells progress through a normal cell cycle. Steady-state

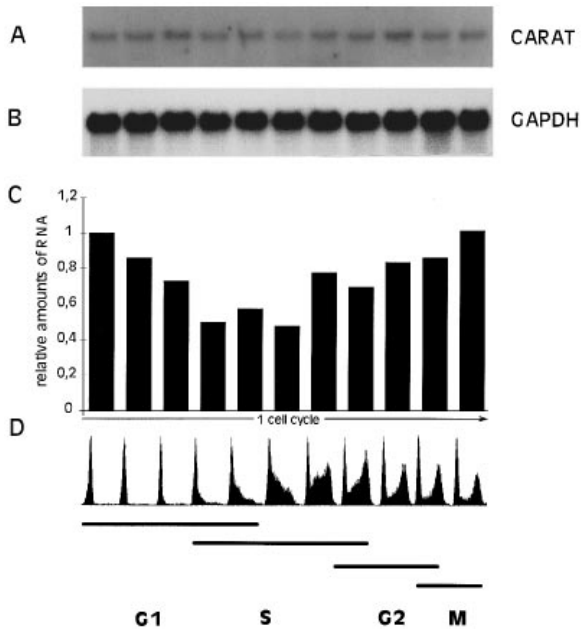

Figure 4 Northern-blot analysis of CARAT mRNA levels as a function of the cell cycle in cycling NIH3T3 cells

Cytoplasmic RNA (10 μg) isolated from NIH3T3 cells at different stages of the cell cycle, separated by centrifugal elutriation, was fractionated on a denaturing gel, transferred and hybridized with random-primed CARAT cDNA (**A**). GAPDH was used as a reference (**B**). The different amounts of CARAT mRNA induction were determined by a densitometric scan (**C**). A fluorescence-activated cell sorting analysis of the elutriated fractions is shown underneath each lane (**D**).

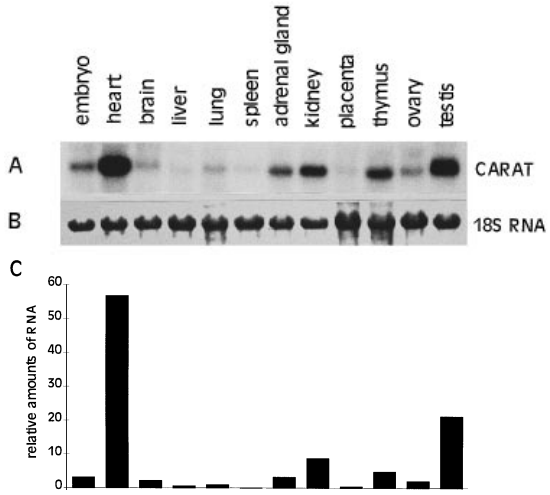

Figure 5 Expression of CARAT in different mouse tissues

Cytoplasmic RNA (10 μg) from the indicated organ isolated by the GTC method was fractionated on a polyacrylamide gel, blotted, and hybridized with random-primed CARAT cDNA (**A**). The relative amounts of RNA were determined by densitometric measurement of the 18 S RNA stained with Methylene Blue and used as a reference (**B**). The murine CARAT is present in all analysed tissues reaching its maximum in heart muscle (56-fold), followed by testis (21-fold), kidney (9-fold) and thymus (5-fold); ratios relative to expression in the liver (**C**). All CARAT expression levels were normalized to the given 18 S RNA signal.

Northern-blot analyses performed with cytoplasmic RNA isolated from cells sorted into cell-cycle fractions by centrifugal elutriation demonstrated very nicely that the murine CARAT

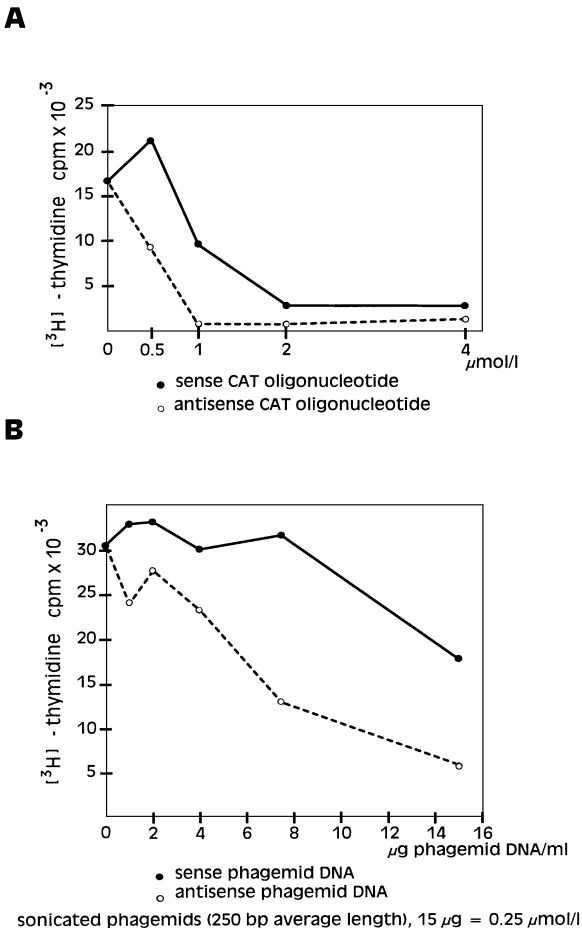

Figure 6 Sense/antisense inhibition studies with CARAT-specific single-stranded ODNs and phagemids

(**A**) Increasing amounts (0 to 4 μmol/l) of single-stranded CARAT-specific ODNs (nt 873 to 892) in sense and antisense orientations were transfected into starved and serum-induced S3T3 mouse fibroblasts. [^{3}H]Thymidine incorporation was assessed 15 h later. (**B**) Sonicated single-stranded phagemids containing the CARAT cDNA in sense and antisense orientations were transfected in different amounts into starved and serum-induced S3T3 cells. The 0 to 15 μg/ml of sonicated phagemids administered give a final single-stranded DNA concentration of 0.25 μmol/l, since the size range of the molecules was 100 to 500 nt according to gel electrophoretic analysis after sonication. Gel analysis and fluorographic measurement of the sonicated phagmids showed that 15 μg of sonicated phagemids with an average length of 0.25 kb resulted in a mean concentration of 0.25 μmol/l in the transfection medium. The [^{3}H]thymidine incorporation as a measure of DNA synthesis was performed as described in the Materials and methods section. The empty phagemid vectors SK$^+$ and SK$^-$ were transfected in the same way and generated an identical [^{3}H]thymidine incorporation curve with values adjacent to the sense phagemid graph (results not shown). All values shown in the diagrams are the means of at least three independent measurements.

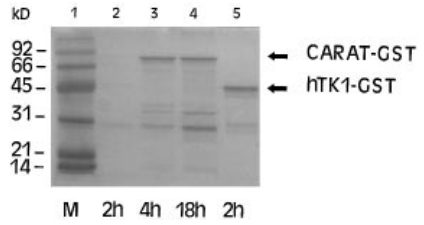

Figure 7 Heterologous expression of the murine CARAT as a GST fusion protein

The CARAT coding region was amplified by PCR and cloned into pGEX-2TK-MCS. Lanes 2–4, lysates from bacterial transformants after 2, 4 and 18 h of induction with IPTG were purified by glutathione–agarose affinity chromatography and separated by PAGE (12% gel). Lane 5, GST–human thymidine kinase 1 (hTK1) fusion protein (2 h of induction) as a control. The arrows indicate major bands of about 77 kDa in lanes 3 and 4 and of 45 kDa in lane 5, respectively, which appear in the Coomassie Blue stained gel and represent the CARAT– and the hTK1–GST fusion proteins with their predicted molecular masses. The induced CARAT–GST fusion protein is hardly visible after 2 h of IPTG induction but appears as a prominent band after 4 and 18 h of IPTG induction (lanes 2–4). The 77 kDa recombinant fusion protein is absent in control lysates isolated from GST expression vectors carrying other eukaryotic proteins like the hTK1 (lane 5). 'Empty' GST expression vectors generate a prominent band at about 30 kDa, which also is visible as a by-product of the bacterial expression system carrying recombinant fusion proteins (personal observation). The molecular masses (kD = kDa) are indicated on the left.

mRNA was induced in a biphasic pattern very similar to the serum induction experiment with a more than 2-fold induction in G1 and G2 over the level in S-phase (see Figure 4). We have also analysed Ehrlich ascites cells for the cycling behaviour of the CARAT mRNA in an unperturbed cell cycle. There the induction was much more pronounced, showing a 6-fold induced transcript level in early G1 compared with S-phase (results not shown); in NIH 3T3 cells the induction was about a factor of 2. This distinct cycling behaviour of the CARAT mRNA is clearly visible in both serum induction experiments presented in Figures 2 and 3. In all our experiments we used either 28 S RNA or GAPDH to control the equal loading and transfer. The various cell cycle fractions were analysed by a Partec PAS-2 cytofluorimeter and the DNA content versus size of the cells is shown in Figure 4 (D).

The tissue distribution shown in Figure 5 demonstrates that the CARAT transcript is present in all organs analysed, but with large variations in abundance. The CARAT transcript showed its highest levels in heart muscle, with 56-fold, followed by the testis with 21-fold, kidney 9-fold and thymus 5-fold above the levels measured in liver, lung and placenta.

Genes emerging from a differential or subtractive hybridization experiment are only characterized by their transcript abundance at the two growth states chosen for the comparison. In order to ascertain the importance of this gene in cell cycle progression or in other cellular processes, we developed a new sense/antisense inhibition approach based on strand-specific single-stranded DNA phagemids carrying the CARAT cDNA clone. In addition, we have delineated sense and antisense ODNs from the CARAT coding sequence and analysed them in a similar way. These experiments showed that S3T3 cells synchronized by serum starvation were progressively inhibited from proceeding into S-phase in the presence of increasing concentrations of 3-1a antisense-specific ODNs. The antisense constructs inhibited more effectively than the sense constructs. Very low [^{3}H]thymidine incorporation was measured at antisense ODN concentrations of 2 μmol/l in the cell culture medium, whereas the sense ODN only caused a reduction of 50% incorporation of radioactivity in this concentration range (Figure 6A). At higher ODN concentrations the [^{3}H]thymidine pools are diluted by unlabelled ODN degradation products and the measured incorporation cannot be directly linked with the proliferative status. The administration of strand-specific phagemids carrying cDNA in both orientations to S3T3 cells *in vivo* worked very satisfactorily and underlined the ODN-derived results (Figure 6B). Throughout the entire concentration range from 1 to 15 μg sonicated phagemids/10^5 cells the antisense construct (pBluescript 3-1aSK+) continuously reduced the incorporation of radioactive label into DNA.

To be able to analyse the encoded protein, we integrated the complete mouse CARAT cDNA in frame into a pGEX-2T vector (Pharmacia) [33]. After induction with isopropyl β-D-

thiogalactopyranoside (IPTG) a glutathione S-transferase (GST) fusion protein could be detected at the expected size (see Figure 7). The GST/CARAT fusion protein was purified by adsorption to glutathione beads and was found to have a molecular mass of 77 kDa. This is consistent with the sequencing data and confirms that clone 3-1a encodes a full-length mouse CARAT. A one-step biochemical purification of the fusion protein by affinity chromatography to glutathione–agarose beads resulted in substantial purification of the recombinant fusion protein.

DISCUSSION

At the beginning our major goal was to develop a sensitive differential screening method that would enable us to identify mRNAs of low abundance that were differentially expressed in eukaryotic cells in G1 and S-phase. During the last 10 years various approaches have been developed to identify mRNAs differentially expressed during the cell cycle or more generally in two cell populations differing by some criterion of interest. When classified by technical terms these approaches are called differential screening, whether based on PCR differential display or subtractive hybridization. All these methods have a common aim: to identify genes whose transcripts are present in different amounts under two different biological conditions [26,38–42]. A critical parameter in all differential screening experiments concerning the cell cycle is the synchrony of the cell population providing the mRNA. Therefore very often growth arrest and cell cycle inhibitors (isoleucine, thymidine, nocodazole) have been preferred to centrifugal elutriation. There is no doubt in theory that the latter would be the best experimental tool to achieve synchrony, but the problem is sharpness. We have utilized the sodium butyrate-caused growth arrest for several reasons. This substance is a very potent blocking substance but reversible in its action in the low mM concentration range and it halts a cell population at any stage in the cell cycle. For the experimental design an important feature of this drug is its reversibility of action. When cells are released from the block by replacement of the butyrate-containing medium with fresh medium they re-enter the growth cycle at the first hour of the G1 phase [36]. The first growth cycle after butyrate release is very similar to the normal growth cycle and the CARAT mRNA is maximal in G1 and G2. The Northern blots shown in Figures 2 to 4 demonstrate this induction behaviour very nicely.

We isolated the mouse CARAT cDNA clone because its mRNA is expressed at a much higher level 15 h after butyrate release compared with 8 h. The fact that the transcript cannot be 'super induced' by cycloheximide suggests that the mouse CARAT transcript is not destabilized during G1 and early S-phase. To support this finding with cycloheximide we assessed the stability of the CARAT mRNA after actinomycin D inhibition of ongoing transcription at 2 and 15 h after serum induction. At these timepoints we have performed actinomycin D chases lasting 30 min, 1 h, 2 h and 4 h. No differences in the half-life for the CARAT mRNA could be determined by this method (results not shown). We infer that the expression is predominantly regulated at the transcriptional level which causes the differences between 8 h (second half of G1 phase) and 15 h (first half of S-phase) results after butyrate release.

After rescreening a S3T3 cDNA library we were able to clone the full-length 2.596-bp cDNA and to identify an open reading frame for the complete CARAT protein. Comparison of the encoded protein sequence with all the currently known CARAT protein sequences demonstrated a high degree of homology, even to distantly related species like *S. cerevisiae* CARAT (see Figure 1).

The CARAT gene belongs to a small group of genes which show such transcriptional activity, where an increase of transcript abundance occurs in late G1 as well as in late G2 causing an elevated steady state level of CARAT mRNA still in early G1. This is the case not only in NIH3T3 cells (Figure 3) but also in S3T3 cells where the differential screening experiment had been performed (Figure 2). The explanation for the biphasic induction behaviour could be found via the involvement of the CARAT gene in the acyl-group transfer from mitochondria into the cytoplasm and peroxisomes and its regulatory influence on β-oxidation. Both G1 and G2 phases are periods of considerable anabolic activity. The CARAT gene function provides the cell with a necessary building block and fuel. Since this basic biological function is indispensable for a proper cellular metabolism it is convincing that this gene function is induced in both G1 and G2 phases.

The enzyme mechanism plays an important role during the regulation of the β-oxidation of fatty acids, since the ratio of CoA versus acetyl-CoA is directly linked with the feedback control of the lipid degradation and with cellular energy production [43]. Via its enzymic activity and intracellular localization the CARAT represents a central function involved in the cellular energy metabolism. Although the biochemical properties of the CARAT enzyme are well known, less is known about its regulation. By cloning the complete and functional cDNA of the mouse CARAT gene we have generated a tool which enabled us to analyse mRNA regulation. The gene itself is known to be involved in the control of the changing energy demand of the heart muscle [44]. The tissue blot demonstrates very clearly a high abundance in this organ (56-fold) compared with other tissues. From this picture we predict a strong diagnostic and pharmacological importance and the need to search specifically for CARAT activity aberrations and transcript amounts in heart muscle deficiencies and in vasoconstrictive and degenerative processes of the arterial blood vessel system.

It has been shown that the CARAT function exhibits a diagnostic decrease in samples derived from patients suffering from Alzheimer's disease [23–25]. In animal studies administration of acetylcarnitine and L-carnitine to animals maximized energy production, promoted cellular membrane stability and restored levels of mitochondrial transcripts in ageing rats [23,45,46]. Damage occurring to brain cells in Alzheimer's disease and in senile dementia of the Alzheimer type is evident and well documented. Improving the long-chain fatty acid 'shuttle' traffic between the cytosol and the mitochondria by administration of acetylcarnitine seems very appealing. But there is an urgent need for further molecular studies, perhaps in early pathological conditions, where this enzyme may serve as a useful diagnostic tool or even could open a new therapeutic concept to improve the severe pathological situation in patients with Alzheimer's disease.

To enhance our differential screening approach we were forced to develop a test system which could tell us more about the biological significance of an unknown novel gene function prior to detailed sequence analysis. It was tempting to administer directly single-stranded phagemids, which had to be sonicated to guarantee equal transfection and intracellular degradation rates. This source of single-stranded CARAT-specific cDNA turned out to work quite effectively. In a continuation of these studies the mouse CARAT cDNA will be stably transformed into mouse fibroblasts: CARAT-specific transcripts can then be induced at selected timepoints of the cell cycle. In our experiments the standard sense/antisense ODNs and the CARAT-carrying phagemids were comparably effective as inhibitors of [^{3}H]thymidine incorporation. Further experiments with senescent

(aging) cells, as well as with cells with a background of mitochondrial pathology, and in tissue samples of patients suffering from Alzheimer's disease (animal model) [47], will bring more insight into the enigma of the biological and the tissue- and organelle-specific role of this enzyme function.

We thank T. Sauer for skilful technical research assistance during the experimental work. Although the initial phase of this research was supported by a grant to D.T.D. from the MRC (Canada) and NCI (Canada), most of the research was supported by a grant to R.H. from the Herzfelder'sche Familienstiftung of the Medical Faculty of University of Vienna. S.B. received a Ph.D. stipendium of the University of Vienna.

REFERENCES

1 Bieber, L. L. and Farrell, S. O. (1983) Carnitine acetyltransferases, in The Enzymes (Boyer, P. D., ed.), vol. 16, pp. 627–644, Academic Press, New York
2 Bieber, L. L. (1988) Annu. Rev. Biochem. **57**, 261–283
3 Chatterjee, B., Song, C. S., Kim, J. M. and Roy, A. K. (1988) Biochemistry **27**, 9000–9006
4 Brice, A., Berrard, S., Raynaud, B., Ansieau, S., Coppola, T., Weber, M. J. and Mallet, J. (1989) J. Neurosci. Res. **23**, 266–273
5 Woeltje, K. F., Esser, V., Weis, B. C., Sen, A., Cox, W. F., McPhaul, M. J., Slaughter, C. A., Foster, D. W. and McGarry, J. D. (1990) J. Biol. Chem. **265**, 10720–10725
6 Finocchiaro, G., Taroni, F., Rocchi, M., Liras-Martin, A., Colombo, I., Tarelli, G. T. and DiDonato, S. (1991) Proc. Natl. Acad. Sci. U.S.A. **88**, 661–665
7 Esser, V., Britton, C. H., Weis, B. C., Foster. D. W. and McGarry, J. D. (1993) J. Biol. Chem. **268**, 5817–5822
8 Kispal, G., Sumegi, B., Dietmeier, K., Bock, I., Gajdos, G., Tomcsanyi, T. and Sandor, A. (1993) J. Biol. Chem. **268**, 1824–1829
9 Corti, O., Finocchiaro, G., Rossi, E., Zuffardi, O. and DiDonato, S. (1994) Genomics **23**, 94–99
10 Johnson, T. M., Kocher, H. P., Anderson, R. C. and Nemecek, G. M. (1995) Biochem. J. **305**, 439–444
11 Elgersma, Y., van Roermund, C. W. T., Wanders, R. J. A. and Tabak, H. F. (1995) EMBO J. **14**, 3472–3479
12 Gadaleta, M. N., Petruzzella, V., Renis, M., Fracasso, F. and Cantatore, P. (1990) Eur. J. Biochem. **187**, 501–506
13 Agius, L., Wright, P. D. and Albert, K. G. (1987) Clin. Sci. **73**, 3–10
14 DiDonato, S., Rimoldi, M., Moise, A., Bertagnolio, B. and Uziel, G. (1979) Neurology **29**, 1578–1583
15 Przyrembel, H. (1987) J. Inherited Metab. Dis. **10**, 129–146
16 Bougneres, P. F., Saudubray, J. M., Marsac, C., Bernard, O., Odievre, M. and Girard, J. (1981) J. Pediatr. **98**, 742–746
17 Bonnefont, J. P., Hass, R., Wolff, J., Thuy, L. P., Buchta, R., Carroll, J. E., Saudubray, J. M., Demaugre, F. and Nyhan, W. L. (1989) J. Child Neurol. **4**, 198–203
18 Demaugre, F., Bonnefont, J. P., Colonna, M., Cepanec, C., Leroux, J. P. and Saudubray, J. M. (1991) J. Clin. Invest. **87**, 859–864
19 Taroni, F., Verderio, E., Fiorucci, S., Cavadini, P., Finochiaro, G., Uziel, G., Lamantea, E., Gellera, C. and DiDonato, S. (1992) Proc. Natl. Acad. Sci. U.S.A. **89**, 8429–8433
20 Ratheiser, K., Schneeweiss, B., Waldhäusl, W., Fasching, P., Korn, A., Nowotny, P., Rohac, M. and Wolf, H. P. (1991) Metab. Clin. Exp. **40**, 1185–1190
21 Wolf, H. P. O. (1992) Horm. Metab. Res. Suppl. **26**, 62–67
22 Makar, T. K., Cooper, A. J., Tofel-Grehl, B., Thaler, H. T. and Blass, J. P. (1995) Neurochem. Res. **20**, 705–711
23 Carta, A., Calvani, M., Bravi, D. and NiBhuachalla, S. (1993) Ann. N.Y. Acad. Sci. **695**, 324–326
24 Kalaria, R. N. and Harik, S. I. (1992) Ann. Neurol. **32**, 583–586
25 Hofbauer, R. and Denhardt, D. T. (1991) CRC Crit. Rev. Eukaryotic Gene Expression **1**(4), 247–300
26 Hofbauer, R. and Denhardt, D. T. (1993) Methods Mol. Genet. **2**, 2–25
27 D'Anna, J. A., Tobey, R. A. and Gurley, L. R. (1980) Biochemistry **19**, 2656–2671
28 Russel, M., Kidd, S. and Kelley, M. R. (1986) Gene **45**, 333–338
29 Gubler, U. and Hoffmann, B. J. (1983) Gene **25**, 263–269
30 Feinberg, A. P. and Vogelstein, B. (1983) Anal. Biochem. **132**, 6–13
31 Sambrook, J., Fritsch, E. F. and Maniatis, T. (1989) Molecular Cloning: A Laboratory manual, Cold Spring Harbor Laboratory Press, Cold Spring Harbor, NY
32 Smith, D. B. and Johnson, K. S. (1988) Gene **67**, 31–40
33 Karlseder, J., Rotheneder, J. and Wintersberger, E. (1996) Mol. Cell. Biol. **16**, 1659–1667
34 Frangioni, J. V. and Neel, B. G. (1993) Anal. Biochem. **210**, 179–187
35 Pearson, W. R. and Lipman, D. J. (1988) Proc. Natl. Acad. Sci. U.S.A. **85**, 2444–2448
36 Wintersberger, E., Mudrak, I. and Wintersberger, U. (1983) J. Cell. Biochem. **21**, 239–247
37 Raghow, R. (1987) Trends Biochem. Sci. **12**, 358–360
38 Lau, L. F. and Nathans, D. (1985) EMBO J. **4**, 3145–3151
39 Sargent, T. D. (1987) Methods Enzymol. **152**, 423–442
40 Almendral, J. M., Sommer, D., MacDonald-Bravo, H., Burckhardt, J., Perera, J. and Bravo, R. (1988) Mol. Cell. Biol. **8**, 2140–2148
41 Parfett, C. L. J., Hofbauer, R., Brudzynski, K., Edwards, D. R. and Denhardt, D. T. (1989) Gene **82**, 291–303
42 Liang, P. and Pardee, A. B. (1992) Science **257**, 967–971
43 Uziel, G., Garavaglia, B. and DiDonato, S. (1988) Muscle Nerve **11**, 720–724
44 Bakker, A., Biermans, W., Van-Belle, H., De-Bie, M., Bernaert, I. and Jacob, W. (1994) Biochim. Biophys. Acta **1185**, 97–102
45 Aureli, T., Miccheli, A., Ricciolini, R., DiCocco, M. E., Ramacci, M. T., Angelucci, L., Ghirardi, O. and Conti, F. (1990) Brain Res. **526**, 108–112
46 Gadaleta, M. N., Petrucella, V., Renis, M., Fracasso, F. and Cantatore, P. (1990) Eur. J. Biochem. **187**, 501–506
47 Makar, T. K., Hungund, B. L., Cook, G. A., Kashfi, K. and Cooper, A. J. (1995) J. Neurochem. **64**, 2159–2168

Received 11 June 1996/23 September 1996; accepted 21 October 1996